Appl. Phys. B 86, 547–553 (2007)
DOI: 10.1007/s00340-006-2532-3

Applied Physics B
Lasers and Optics

S.S. HARILAL✉
B. O'SHAY
Y. TAO
M.S. TILLACK

Ion debris mitigation from tin plasma using ambient gas, magnetic field and combined effects

Center for Energy Research, University of California, San Diego, 9500 Gilman Drive, La Jolla, CA 92093-0438, USA

Received: 19 June 2006/Revised version: 30 October 2006
Published online: 15 December 2006 •

ABSTRACT Mitigation of energetic ions from laser produced tin plasma is one of the principal issues in the development of an extreme ultraviolet lithographic light source. We explored the possibility of using an ambient gas and/or a magnetic field for controlling the energetic ions from tin plasma. Hydrogen, helium and argon gases provide good transmission to 13.5 nm and are found to be an effective stopper for tin ions. Absorption of in-band radiation limits the density of gas below levels needed to completely protect optics. Tin ion ranges in buffer gases were estimated using the Monte Carlo simulation code SRIM and compared with experimental results. The presence of a moderate transverse magnetic field of 0.64 T slowed the propagation of fast moving tin ions but failed to stop them. The synergistic effect of a combination of magnetic field and an ambient gas is found to be very promising for mitigating tin ions without exceeding EUV gas absorption limits.

PACS 42.72.Bj; 52.50.Jm; 52.55.Jd; 52.70.kz

1 Introduction

Extreme ultraviolet lithography (EUVL) is a leading candidate for next generation high volume patterning that requires feature sizes less than 32 nm. The essential requirement for enabling this technology is to have a reliable, clean and powerful light source around 13.5 nm. The choice of wavelength is based on the strong emission line of Li at 13.5 nm and the availability of Mo/Si multi-layer mirrors that reflect more than 70% of the in-band radiation centered at 13.5 nm with 2% bandwidth. A laser-produced plasma (LPP) EUV source has a strong potential to be the future light source. Laser generated plasma from lithium, xenon, tin and water are good emitters in the in-band region of the spectral curve [1–4] and tin plasma is more promising in this context as it provides higher conversion efficiency (CE) than lithium or xenon [5, 6]. However, a condensable target like tin can pose extreme debris problems in commercial lithography processes. The debris from LPP includes energetic ions and neutrals, particulates and molten droplets. Controlling or mitigating the debris has been attempted by various groups using different methods, including cavity confined plasma [7], tape targets [8], mass limited droplet targets [9, 10], foil trap [11], the application of electrostatic repeller fields [12], and magnetic fields [13, 14].

An ambient gas can be used as a moderator or stopper for highly energetic tin ions and hence can be an effective way to mitigate debris. Bollanti et al. [15] used krypton for controlling debris from a laser- produced Ta plasma and their results showed that the ambient gas significantly reduced debris at the witness plate. However, care must be taken in selecting a proper ambient environment for an EUVL source set-up since most gases absorb EUV photons. Hydrogen, helium and argon provide exceptionally good transmission to 13.5 nm compared to other gases [16]. Recently, we reported the dynamics of tin plumes in the presence of argon ambient using optical emission spectroscopy [17]. We noticed, apart from thermalization and deceleration of plume species, that the addition of ambient gas leads to other events such as double peak formation in the temporal distributions and ambient plasma formation.

It is well known that a magnetic field interacts with charged particles in a plasma and hence can be utilized for controlling ions. It has been postulated [18] that a cloud of laser-produced plasma will be stopped by a magnetic field B in a distance $R \sim B^{-2/3}$. In addition to confinement, the presence of a magnetic field may lead to ion acceleration, enhanced emission intensity, and various kinds of instability [19]. Recently we investigated the influence of magnetic fields on the confinement and dynamics of the plume using fast photography and optical emission spectroscopy [19, 20]. A moderate transverse magnetic field of 0.64 T is found to be very effective for inhibiting expansion of the plume from low $\langle Z \rangle$ materials like carbon [20] and aluminum [19], while the field showed only deceleration of excited ions and neutrals from laser produced Sn plasma [13]. These studies showed that even though the Larmor radii of the electrons and Sn ions are a few micrometers and centimeters respectively, the plume propagates without stopping. It suggests the plasma should be treated as a fluid rather than considering individual particles.

In this paper, we report the effectiveness of ambient gases and magnetic fields for moderating and stopping fast tin ions. The gases used for containing tin ions are hydrogen, helium

✉ Fax: +1+858-822-2120, E-mail: Harilal@fusion.ucsd.edu

and argon as they are less absorptive to in-band radiation. The projected range of the tin ions at different pressure levels was estimated using a Monte Carlo simulation code of the stopping power and ranges of ions in matter [21]. A Faraday cup is used for measuring the tin ion flux placed at a distance ~ 15 cm from the target surface. An absolutely calibrated EUV calorimeter is used for measuring in-band conversion efficiency. A transverse magnetic field of 0.64 T showed minimal effect on tin ion propagation. However, a synergistic effect, such as a combination of a moderate magnetic field and a low-pressure buffer gas, is found to be very effective for mitigating tin ions without penalizing EUV photon absorption by the ambient gas.

2 Experimental

For producing tin plasma, 1064 nm, 10 ns (full width at half maximum, FWHM) pulses from an Nd:YAG laser was used. The target was placed in a stainless steel vacuum chamber that is pumped using a cryogenic pump and a base pressure of $\sim 10^{-6}$ Torr was easily achieved. The laser beam, at normal incidence, was focused on to the target using a plano-convex lens to a focal spot diameter of 60 µm. The focal spot at the target surface was measured using an optical imaging technique and remained unchanged during the experiment. A 2 mm thick tin target in the form of a slab was translated to provide a fresh surface for each shot to avoid errors associated with local heating and drilling. The ion emission has been monitored using a Faraday cup placed at a distance 15 cm from the target surface. The ion current was measured by acquiring the voltage signal across a load resistor by a 500 MHz digital phosphor oscilloscope.

The transverse magnetic field is supplied by an assembly of two permanent magnets mounted in a steel core to create a maximum field of 0.64 T over a volume 5 cm × 2.5 cm × 1.5 cm. The target is placed 1 cm from the pole edges creating a uniform magnetic field along the plume expansion direction.

A transmission grating spectrograph with a back illuminated CCD was used for recording the EUV spectra in the wavelength range 5–20 nm. An absolutely calibrated EUV calorimeter (E-Mon, JenOptik Mikrotechnik, Jena) was used for measuring the CE of the in-band radiation at 13.5 nm with 2% bandwidth. The principle of operation of the energy monitor is filtering out the in-band range from the broadband incidence spectrum of the EUV source by using a Zr filter (it suppresses the radiation above 50 nm) and two Mo/Si multilayer mirrors (for filtering in-band radiation). A photodiode (IRD, SUXV-100) that is sensitive to the EUV range is used for detection. Both the spectrograph and the energy monitor were placed at 45° with respect to the laser beam.

3 In-band transmission in gases

We selected argon, helium and hydrogen gases as the ambient because they possess exceptionally good transmission to in-band radiation. Typical transmission for 13.5 nm radiation at different argon and helium pressures is given in Fig. 1 for a path length of 15 cm [16]. The selection of path lengths in the figure is based on the fact that in an EUVL tool, the collector mirror is expected to be placed ~ 15–20 cm

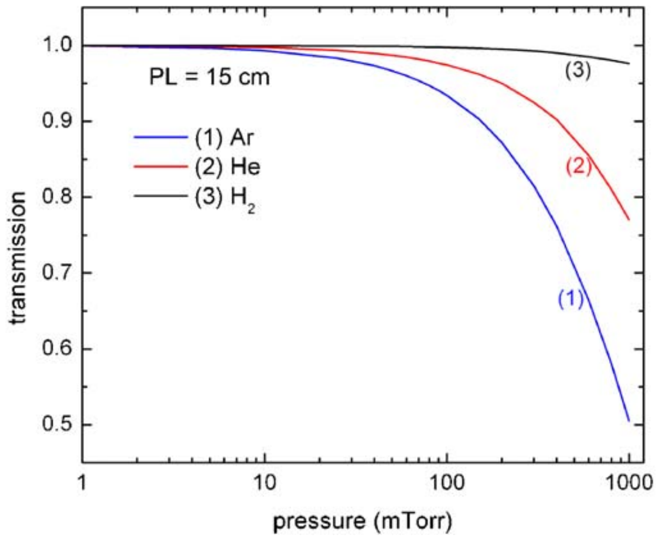

FIGURE 1 Transmission of 13.5 nm radiation at different argon and helium pressures is given for a path length of 15 cm

from the plasma. X-ray transmission studies showed that more than 90% of the 13.5 nm radiation is transmitted for a path length of 15 cm when the argon and helium pressures are less than 100 and 300 mTorr respectively, while hydrogen provides exceptionally good transmission to in-band radiation even at pressure levels of a few Torr.

4 Stopping distance and range

The mean projected length of tin ions at different argon ambient pressures was estimated using the Monte Carlo simulation program SRIM [22]. SRIM calculates the stopping and range of ions (10 eV–2 GeV/amu) into matter using a full quantum mechanical treatment of ion-atom collisions. A full description of the SRIM calculation can be found in [21]. Fig-

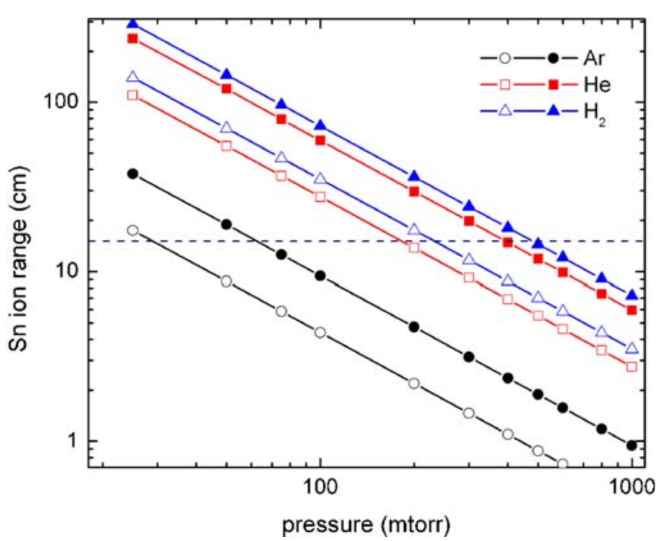

FIGURE 2 The SRIM estimate of the flight range of tin ions with different values of initial energies propagating into an ambient gas is shown. The *hollow symbols* correspond to a starting energy of 1 keV and the *darkened symbols* are for 5 KeV. The *dashed line* in the center corresponds to the Faraday cup position (15 cm)

ure 2 shows the theoretical calculation of the flight range of tin ions with different values of starting energies propagating into argon, helium and hydrogen ambient with various pressure levels. The dashed line at the center of the figure corresponds to the position of the Faraday cup.

As can be seen in Fig. 2, at any value of pressure and energy of ion, the argon buffer stops the tin ions in a spatial range approximately 6.3 times shorter than helium and 8 times shorter than H_2. It also shows that with a 63 mTorr argon pressure, the ions with kinetic energies ≤ 5 keV can be effectively stopped before reaching the collector mirror placed at 15 cm. The flight range estimations with helium and hydrogen showed that a pressure of about 395 mTorr and 485 mTorr respectively is necessary for stopping tin ions before reaching the detector placed at 15 cm. Under these pressure conditions helium is found to be more absorptive to 13.5 nm radiation than argon at 63 mTorr. However, H_2 at 485 mTorr is more transparent to in-band radiation. It should be remembered that SRIM doesn't consider the collisionality of the plasma. So the effective experimental stopping distance may be different compared to SRIM analysis. Hence an experimental comparative study with argon, helium and hydrogen as the buffer is necessary to obtain more insight into this context.

5 Sn plume characteristics in vacuum

Tin plasmas characteristically emit broadband spectra around 13.5 nm that come from many excited levels of different ionization stages. These energy levels are so close that the radiation they generate in the EUV range can be considered as a continuum (unresolved transition array, UTA). The UTA emission is concentrated around 13.5 nm with a narrow band gap of 5–10 eV arising from $4p^64d^n - 4p^54d^{n+1} + 4p^64d^{n-1}4f$ transitions of various Sn ions ranging from Sn^{6+} to Sn^{14+} with occupancy in the range of $n = 2$ to $n = 8$ [23]. Typical UTA emission obtained from Sn plasma is shown in Fig. 3. Our EUV spectral measurements showed the UTA brightness was maximum when the laser irradiance reaches $\sim 4\times10^{11}$ W cm^{-2} with a spot size of 60 μm [4]. Above the optimal laser irradiance, a greater portion of the radiated energy appears at shorter wavelengths, and at lower irradiance levels the plasma is insufficiently heated to emit at 13.5 nm. At the optimal laser irradiance level the ionization balance of the plasma shifts toward Sn^{9+} to Sn^{12+} which contributes primarily to in-band UTA radiation [4]. So we kept the laser intensity at 4×10^{11} W cm^{-2} for all the measurements. The estimated conversion efficiency (CE, 13.5 nm with 2% bandwidth) at these laser intensities approaches a value of 2%.

A typical TOF ion signal recorded using the Faraday cup in vacuum is given in Fig. 4. The Faraday cup is positioned at a distance 15 cm from the target surface and 12° to the target normal. The ion TOF profile in vacuum is represented by a sharp prompt peak followed by a broad slower peak. The fast prompt peak in the ion signal is caused by photoelectric effect and can be used as a time marker. The estimated expansion velocity using the peak of the TOF of positive ions is $\sim 4.3\times10^6$ cm s^{-1}. The kinetic energy distribution of tin ions in vacuum is also given in the inset of Fig. 4. The kinetic energy spectra showed the tin ions distributed in the energy region up to 5 keV with maximum ion flux at 1.1 keV. The kinetic energy distributions can usually be described by a shifted Maxwell–Boltzmann (SMB) distribution. A SMB fits fairly well with the KED curve as shown in Fig. 3.

The ion measurements mentioned above are carried out at 12° with respect to the target normal. It should be noted that the distribution of ions in a laser created plasma are best approximated by single charge dependent $\cos^n$ function where the value of n increases with charge state and decreases with atomic mass [24]. The ions of highest ionization state dominate in the direction normal to the target, and their concentration falls sharply away from the normal and excited neutrals have got the most angular spread. It can be due to the fact that charge density at outer angular regions of the plume is effectively diminished by recombination.

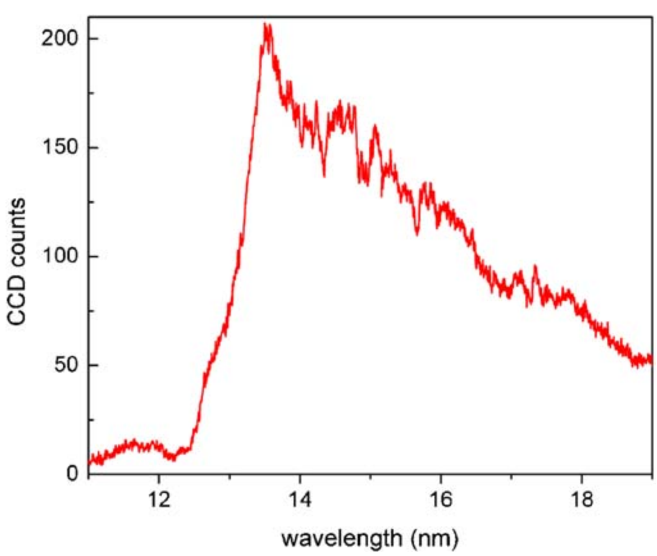

FIGURE 3 UTA from laser produced Sn plasma. The laser intensity used is 4×10^{11} W cm^{-2}

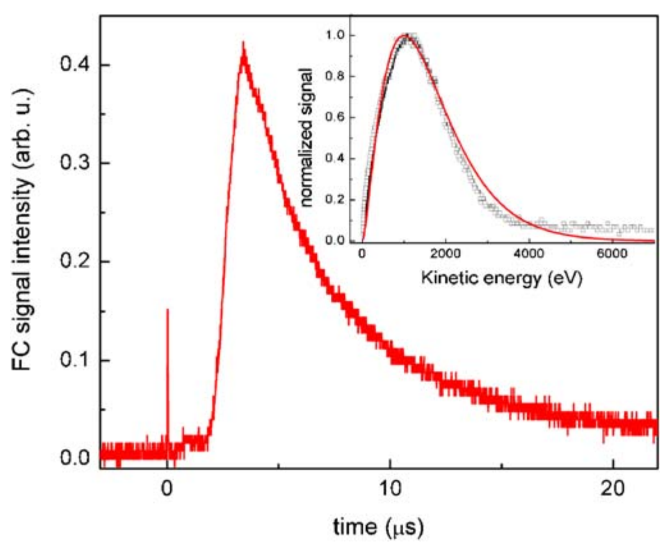

FIGURE 4 TOF of ions recorded using a Faraday cup placed at a distance ~ 15 cm from the target surface for plume expansion into vacuum. The kinetic distribution of the tin ions obtained from TOF signal in vacuum is given in the *inset*. The *solid line* represents the SMB fit and *points* represent experimental data points

6 Ion mitigation using ambient gases

The addition of ambient gas usually affects the kinetic distribution of all species in the plume because of plume–buffer interaction [25, 26]. Gas phase collisions can transform the initial temporal distributions into a very different final distribution. The plume expansion into vacuum is adiabatic and treated well by Anisimov et al. [27]. The interaction of the plume with an ambient gas is a far more complex gas dynamic process that involves deceleration, attenuation, and thermalization of the ablated species, as well as the formation of shock waves [28, 29]. Our studies also revealed plume splitting in a laser created aluminum plasma expanding into an ambient air environment where gas phase collisions transformed the initial temporal distribution into a very different final distribution [28]. We distinguished three distinct pressure regimes using fast photography, each of which is characterized by a particular behavior of the plume. At low pressure or in vacuum, the plume expands freely without any external viscous force. At intermediate pressure levels (transition regime), the plume is characterized by strong interpenetration of the plasma species and background gas that leads to plume splitting and sharpening. At high pressures, due to enhanced collisions with the background gas species, the deceleration process is very rapid and eventually plume propagation stops and particles become thermalized.

Based on the modeling by Westwood [30] of the scattering of sputter atoms by an ambient gas, an Sn atom in collision with an argon atom changes its direction by $\approx 16°$ and loses $\approx 40\%$ of its kinetic energy while with a collision with an helium atom, Sn changes its direction by $\approx 1.6°$ and loses 5% of its energy. Being a lighter gas, the loss of energy by a Sn atom in collision with H_2 is much less. It indicates that a higher helium or hydrogen gas density is necessary for controlling tin species in comparison with argon. However, these estimations are based on the assumption that Sn atoms are travelling normal to the target and hence it may not be true for a collective fluid medium like laser-produced plasma.

The ion time of flight signals are recorded with three different gases and at various pressure levels. Typical TOF profiles of Sn ions at different argon pressure levels are given in Fig. 5. Figure 6 shows the integrated yield of Sn ions as a function of gas pressure. It provides an indication of mitigation of ion species with increasing buffer gas pressure. The data show that the ion flux reduces rapidly when the ambient argon pressure increases from 10 to 50 mTorr. It also shows that approximately 70 mTorr argon pressure is enough for mitigation of tin ions if the collector mirror is placed around ~ 15 cm from the target surface, which is in good agreement with theoretical prediction by SRIM code. The measured ion flux in the presence of helium ambient showed a slower decrease with increasing pressure compared to argon due to its lighter mass. A helium pressure of ~ 400 mTorr is needed for mitigating tin ions, which also agrees well with SRIM prediction. Hydrogen ambient also showed similar pressure levels to helium for stopping even though SRIM predicted slightly higher values (485 mT). The argon and helium ambient gas stopping is found to be marginal considering the in-band photon absorption by the gas. Hydrogen ambient is more suitable for mitigating Sn ions as the pressure levels required for stoppage of tin ions is more transparent to in-band radiation compared to argon and helium buffer.

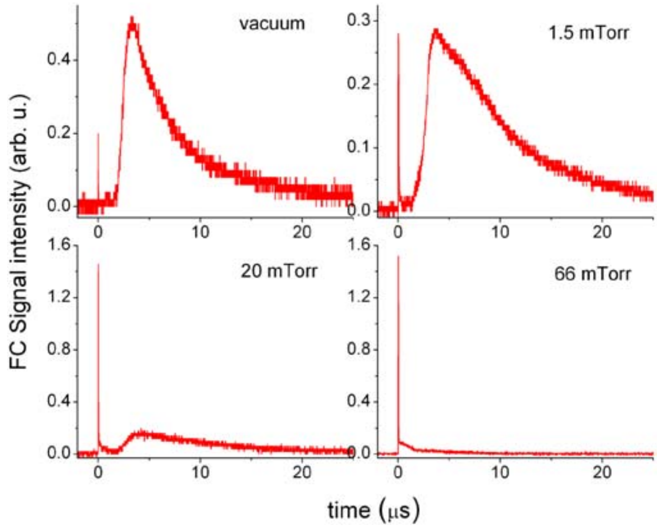

FIGURE 5 The TOF profiles of tin ions at different argon pressures are given

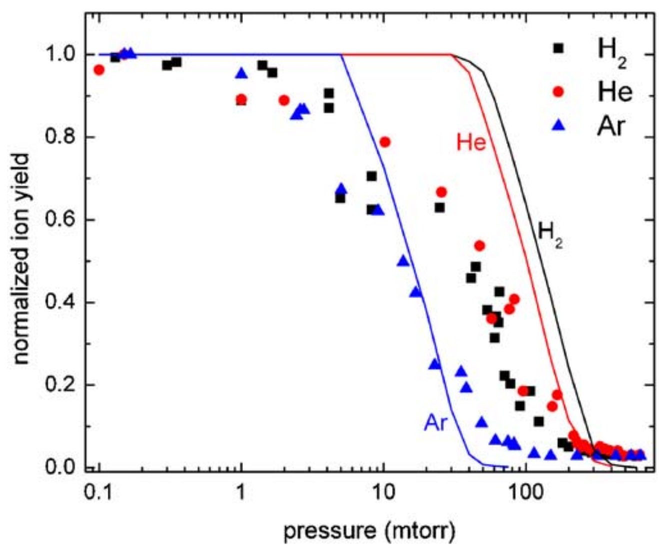

FIGURE 6 Integrated ion yield obtained from Faraday cup TOF ion data at different gas pressure levels of argon, helium and hydrogen. The *solid curves* correspond to ions yield obtained from SRIM

The TOF profiles showed that most of the ions are quenched before reaching the collector plate at higher pressures. However, an additional sharp peak with short arrival time is observed in the presence of ambient gas. The sharp peak appears when the buffer gas pressure is greater than 1 mTorr and its intensity increases monotonically with pressure until the pressure reaches 30 mTorr. This is presumably caused by the presence of ambient plasma excited by prompt electrons in the vicinity of the charge collector system [17]. There exists some reports over the excitation and ionization of ambient gas caused by the prompt electron ejected during early time of laser matter interaction [31, 32]. The prolonged decay time of the sharp peak is due to various lifetimes of excited states involved in the argon excitation and ionization [17].

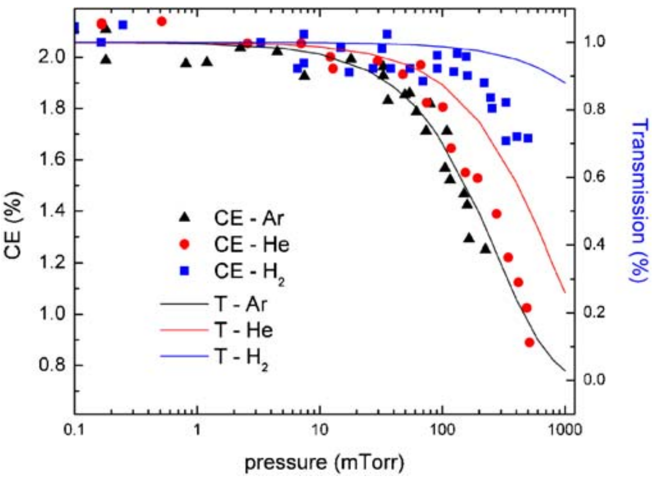

FIGURE 7 The variation with CE with buffer pressure is given. The *symbols* represent the experimental data points and the *curves* give the 13.5 nm transmission (T) at different gas pressures for a path length of 78 cm

The EUV in-band energy was measured using the energy monitor in a well-defined solid angle, which was determined by an aperture and its distance from the source along the beam path. The absolutely calibrated detector used in the calorimeter is placed 78 cm from the plasma source. Since the EUV plasma emission has got an approximately hemispherical symmetry, the output from the energy monitor was simply integrated over a 2π solid angle. The variation of the CE signal with ambient gas pressure is given in Fig. 7. The transmission properties of 13.5 nm for a path length of 78 cm is also given in the figure as it corresponds to the distance from the plasma source to the EUV detector in our experimental set up. The CE measurements showed that the H_2 ambient is more favorable compared to Ar or He gases as it has less absorption to in-band energy where gas mitigation is effective. The use of hydrogen ambient as a stopper may invite some safety standards as it is highly flammable. Since the estimated required pressure of the hydrogen for stopping ions is less than 1 Torr, it will not be a problem considering the safety issue. Now a days, hydrogen has been routinely used in chemical, food and electronic industries in large quantities with a remarkable track record of safety.

7 Magnetic field effects

Investigations also were made with a moderate transverse magnetic field of 0.64 T for controlling or diverting plasma ions. Our previous studies with low $\langle Z \rangle$ materials like carbon and aluminum showed this moderate magnetic field is very effective for controlling the plume. A detailed quantitative description of plume expansion dynamics and confinement in the presence of a transverse magnetic field can be found in [19]. Optical time of flight studies (OTOF) showed that neutrals along with ions can be efficiently controlled by the magnetic field due to confinement of the plume [19]. The ion debris measurements were carried out in the presence of a magnetic field using a Faraday cup placed at 15 cm from the target and at an angle approximately 12° with respect to the target normal. For applying the magnetic field, the target is placed at a distance of 1 cm from the pole edges resulting in a uniform magnetic field along the plume's expansion direction [19].

The kinetic energy distribution of the tin ions showed energies up to 5 keV with a peak ion flux at 1.2 keV. The ion signal obtained in the presence of a magnetic field is given in Fig. 8. It illustrates that the tin ions are considerably slowed down, but not stopped before reaching the Faraday cup. The important parameters that affect the plasma propagation in the presence of a magnetic field are Larmor radius, thermal beta and directed beta. The Larmor radius is proportional to the mass and velocity of the ions and inversely proportional to the charge state and magnetic field strength. Since the Faraday cup does not distinguish between the charge states of different ions collected, it is difficult to estimate the Larmor radius of the ions with various charge state. The estimated Larmor radius for singly ionized Sn is ~ 8 cm and its value decreases with increasing charge state. The Larmor radius of the electrons is $\sim$ μm in dimension. Even though the Larmor radii of ions are much less than the detector distance from the target surface, our studies showed that the applied magnetic field did not stop the ions. It shows plasma should be treated as a fluid rather than considering independent particles alone.

In order to stop plasma propagation across a magnetic field, the beta (β) of the system should be ≤ 1 where β is the ratio of plasma pressure to magnetic pressure. When a plume expands into the magnetic field, the B field exerts a pressure on the fluid composed of charged particles that is given by $P_B = B^2/2\mu_0$. For $B = 0.64$ T, P_B is 1.6 atm. The plasma pressure is contributed to by thermal as well as directed pressure. The thermal pressure of the plume is given by $P_T = nkT$. In the initial time the thermal pressure is expected to be a few thousand atmospheres and its value drops very rapidly because of plume expansion. For example, its value approaches 1 atm at a time 100 ns after the onset of evolution of the plume. We estimated this value using the temperature and density 1.5 eV and 4×10^{17} cm^{-3} respectively, measured by optical spectroscopic means [33]. However, in the later stages, the increase in kinetic energy occurs by direct conversion from elec-

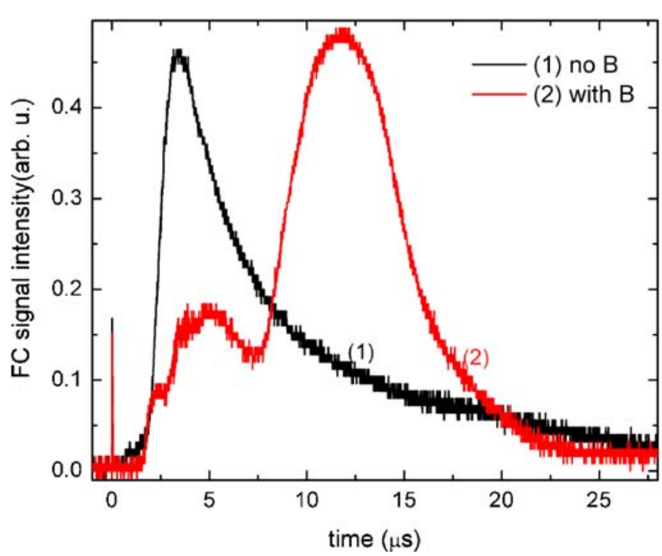

FIGURE 8 The Faraday cup ion signal recorded in the presence and absence of a magnetic field

tron thermal energy, the directed pressure caused by the plume species is important. The directed pressure of the plume is given by $P_d = nmv^2/2$ and its value changes by several orders during plume expansion. The plume will be stopped when the magnetic pressure equilibrates with the plasma pressure (thermal pressure + directed pressure). Using the ion velocity obtained from the Faraday cup, the plume will be effectively stopped when the density approaches $8 \times 10^{14}\,\mathrm{cm}^{-3}$. By assuming the initial density of the plume $\sim 10^{20}\,\mathrm{cm}^{-3}$, the estimated plume density will be $3 \times 10^{14}\,\mathrm{cm}^{-3}$ at 15 cm from the target surface by assuming spherical expansion. Still our ion measurements showed that the magnetic field effectively slowed down the ion propagation rather than stopping it. This disagreement is reasonable since a plasma is a compressible fluid. It shows that a higher magnetic field is necessary for complete ion mitigation.

8 Synergistic effects (combined effect of ambient gas and B field)

All the gases studied showed impressive performance at pressure levels where the in-band transmission is around 90% for a path length of 15 cm. However, these pressure levels are not acceptable in a practical EUVL system because of the absorption of in-band photons by the gas. Even though higher pressures are needed with H_2 ambient for Sn ion mitigation, it transmits more EUV in-band energy compared to argon and helium. Also a moderate magnetic field of 0.64 T showed minimal effect on tin ion propagation. The 0.64 T is found to be effective only in slowing down the ions, but failed to mitigate it. So we tried a combination of a 0.64 T transverse magnetic field and a partial pressure of ambient gas. Typical ion signals recorded with a combination of a 0.64 T magnetic field and a partial pressure of hydrogen are given in Fig. 9. For mitigating Sn ions, the required pressure levels in the presence of magnetic field are 24 ± 4 mT, 67 ± 5 mT and 126 ± 7 mT respectively for Ar, He and H_2 ambient. These results are very promising as the ambient transmission at these pressure levels are more than 98% with a path length of 15 cm.

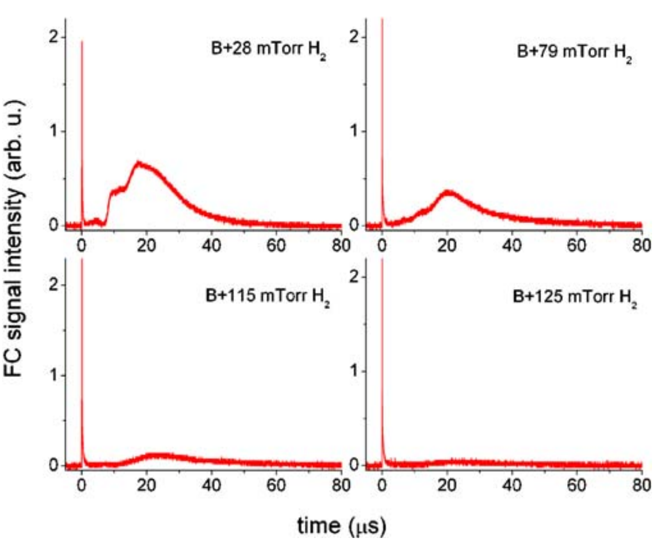

FIGURE 9 Faraday cup ions signal in the combined effect of a magnetic field and ambient gas

It is very difficult to understand the physics behind the synergistic effects of the ambient gas and magnetic field on controlling the ions from the tin plume. One scenario is the magnetic field applied in the vicinity of the plasma simply slowed down the plume species and hence reduced the ambient pressure necessary to stop the ion propagation (no synergistic effect). The other scenario is that the addition of ambient gas enhances the presence of electrons through the formation of ambient plasma even before the arrival of tin plume ions. Our previous studies showed that the laser plasma from tin is preceded by partially ionized ambient gas plasma created by prompt electron excitation and ionization [17]. Hence the presence of an ambient plasma leads to more efficient confinement of the plume as it interacts with laser produced plasma from tin, in the presence of a magnetic field. To prove these arguments, more detailed studies are necessary.

9 Conclusions

Ion debris mitigation in a laser-produced tin plasma is one of the most important issues that must be resolved before implementing them as an EUVL light source. We employed different methods to mitigate the ions coming from Sn plasma, including ambient gases, a magnetic field and a combination of both (synergistic effects).

The selection of argon, helium and hydrogen gases is based on the fact that they have good transmission to in-band radiation compared to other gases. Monte Carlo simulation results showed that with 63 mTorr argon, the tin species with kinetic energies less than 5 keV could be effectively stopped before reaching the collector mirror in an EUVL source set-up, while higher pressures are needed for helium (~ 400 mTorr) and hydrogen (~ 485 mTorr). The ambient gas stopping is found to be marginal considering the in-band photon absorption by the gas. Nevertheless, hydrogen can be used as a stopper for tin ions as the required pressure levels of hydrogen is more transparent to in-band radiation compared to argon and helium. A moderate magnetic field of 0.64 T is found to slow down the ions but failed in stopping them. A combination of an ambient gas and a magnetic field is found to be more promising. For example, a hydrogen pressure of 126 mT is necessary to mitigate tin ions in the presence of a 0.64 T magnetic field and at these pressure levels the in-band radiation is almost unattenuated.

REFERENCES

1 C. Rajyaguru, T. Higashiguchi, M. Koga, K. Kawasaki, M. Hamada, N. Dojyo, W. Sasaki, S. Kubodera, Appl. Phys. B **80**, 409 (2005)
2 C. Rajyaguru, T. Higashiguchi, M. Koga, W. Sasaki, S. Kubodera, Appl. Phys. B **79**, 669 (2004)
3 H. Komori, Y. Ueno, H. Hoshino, T. Ariga, G. Soumagne, A. Endo, H. Mizoguchi, Appl. Phys. B **83**, 213 (2006)
4 S.S. Harilal, B. O'Shay, Y. Tao, M.S. Tillack, A. Nikroo, C.A. Back, J. Phys. D **39**, 484 (2006)
5 S.S. Harilal, M.S. Tillack, Y. Tao, B. O'Shay, R. Paguio, A. Nikroo, Opt. Lett. **31**, 1549 (2006)
6 A. Cummings, G. O'Sullivan, P. Dunne, E. Sokell, F. O'Reilly, J. Phys. D **39**, 73 (2006)
7 T. Tomie, T. Aota, Y. Ueno, G. Niimi, H. Yashiro, J.Q. Lin, I. Matsushima, K. Komiyama, D.H. Lee, K. Nishigori, H. Yokota, Proc. SPIE **5037**, 147 (2003)

8 S.J. Haney, K.W. Berger, G.D. Kubiak, P.D. Rockett, J. Hunter, Appl. Opt. **32**, 6934 (1993)
9 M. Richardson, C.S. Koay, K. Takenoshita, C. Keyser, M. Al-Rabban, J. Vac. Sci. Technol. **22**, 785 (2004)
10 K. Takenoshita, C.S. Koay, S. Teerawattanasook, M. Richardson, V. Bakshi, Proc. SPIE **5751**, 563 (2005)
11 J. Pankert, R. Apetz, K. Bergmann, A. List, M. Loeken, C. Metzmacher, W. Neff, S. Probst, Proc. SPIE **5751**, 260 (2005)
12 C. Koay, S. George, K. Takenoshita, R. Bernath, E. Fujiwara, M. Richardson, V. Bakshi, Proc. SPIE **5751**, 279 (2005)
13 S.S. Harilal, B. O'Shay, M.S. Tillack, J. Appl. Phys. **98**, 036 102 (2005)
14 G. Niimi, Y. Ueno, K. Nishigori, T. Aota, H. Yashiro, T. Tomie, Proc. SPIE **5037**, 370 (2003)
15 S. Bollanti, F. Bonfigli, E. Burattini, P. Di Lazzaro, F. Flora, A. Grilli, T. Letardi, N. Lisi, A. Marinai, L. Mezi, D. Murra, C. Zheng, Appl. Phys. B **76**, 277 (2003)
16 http://www-cxro.lbl.gov/optical_constants/gastrn2.html
17 S.S. Harilal, B. O'Shay, Y. Tao, M.S. Tillack, J. Appl. Phys. **99**, 083 303 (2006)
18 D.K. Bhadra, Phys. Fluids **11**, 234 (1968)
19 S.S. Harilal, M.S. Tillack, B. O'Shay, C.V. Bindhu, F. Najmabadi, Phys. Rev. E **69**, 026 413 (2004)
20 S.S. Harilal, B. O'Shay, M.S. Tillack, C.V. Bindhu, F. Najmabadi, IEEE Trans. Plasma Sci. **33**, 474 (2005)
21 J.F. Ziegler, J.P. Biersack, U. Littmark, *The Stopping and Range of Ions in Solids* (Pergamon Press, New York, 1985)
22 http://www.srim.org
23 A. Cummings, G. O'Sullivan, P. Dunne, E. Sokell, N. Murphy, J. White, K. Fahy, A. Fitzpatrick, L. Gaynor, P. Hayden, D. Kedzierski, D. Kilbane, M. Lysaght, L. McKinney, P. Sheridan, J. Phys. D **37**, 2376 (2004)
24 A. Thum-Jager, K. Rohr, J. Phys. D **32**, 2827 (1999)
25 S.S. Harilal, Appl. Surf. Sci. **172**, 103 (2001)
26 S.S. Harilal, *Advances in Laser and Optics Research*, ed. by W.T. Lavworth (Nova Science, New York, 2002)
27 S.I. Anisimov, D. Bauerle, B.S. Lukyanchuk, Phys. Rev. B **48**, 12 076 (1993)
28 S.S. Harilal, C.V. Bindhu, M.S. Tillack, F. Najmabadi, A.C. Gaeris, J. Appl. Phys. **93**, 2380 (2003)
29 S.S. Harilal, C.V. Bindhu, M.S. Tillack, F. Najmabadi, A.C. Gaeris, J. Phys. D **35**, 2935 (2002)
30 W.D. Westwood, J. Vac. Sci. Technol. **15**, 1 (1978)
31 S. Amoruso, M. Armenante, R. Bruzzese, N. Spinelli, R. Velotta, X. Wang, Appl. Phys. Lett. **76**, 249 (2000)
32 R.C. Issac, G.K. Varier, P. Gopinath, S.S. Harilal, V.P.N. Nampoori, C.P.G. Vallabhan, Appl. Phys. A **67**, 557 (1998)
33 B. O'Shay, F. Najmabadi, S.S. Harilal, M.S. Tillack, J. Phys. Conf. Series (2007), in press